Published by :
http://www.ijert.org

International Journal of Engineering Research & Technology (IJERT)
ISSN: 2278-0181
Vol. 10 Issue 01, January-2021

Stability of Flexibly Supported Finite Oil Journal Bearing Considering Fluid Inertia Effect and Influence of Pressure Dependent Variable Viscosity

A. K. Bandyopadhyay[1]
Assistant Professor,
Department of Mechanical Engineering,
DR. B.C Roy Engineering College, Durgapur,
West Bengal, India

S. K. Mazumder[2]
Professor,
Department of Mechanical Engineering,
DR. B.C Roy Engineering College, Durgapur,
West Bengal, India

Abstract- **The aim of this study is to analyse the Nonlinear transient stability of finite oil journal bearing including the effect of fluid inertia and pressure dependent viscosity. The theoretical analysis is intended to show the effect of fluid inertia with pressure dependent variable viscosity on the journal bearing performance for three-dimensional bearing geometries. The average Reynolds equation is modified to include the fluid inertia effect and variable viscosity effect and is used to obtain pressure field in the fluid-film. The solutions of modified average Reynolds equations are obtained using finite difference method and appropriate iterative schemes. This investigation deals with the stability of flexibly supported finite oil journal bearing with fluid film inertia effect and pressure dependent viscosity. An attempt has been made to evaluate the critical mass parameter. A Nonlinear time transient method is used to simulate the journal centre trajectory to estimate the stability parameter, which is a function of speed.**

In the present work, the modified average Reynolds equation considering the effect of fluid inertia along with the effect of pressure dependent variable viscosity is solved by finite difference method with successive over-relaxation scheme (Gauss-Siedel), while the equation of motion of both journal an bearing are solved by the fourth order Runge - Kutta method. It was observed that the stability increases with the increase in eccentricity ratio, viscosity parameter and modified Reynolds number and also increases with the increase of slenderness ratio.

Keyword: Modified Reynolds number, viscosity parameter, stability, critical mass parameter, fluid film inertia.

I INTRODUCTION

The basic assumptions in the classical hydrodynamic theory include negligible fluid inertia forces in comparison to the viscous forces. Pinkus and Sterlincht [1], have shown that the fluid inertia effect cannot be neglected when the viscous and the inertia forces are of the same order of magnitude. In recent times synthetic lubricants, low viscosity lubricants, are used in industries and owing to high velocity it is possible to arrive at such a situation where flow is laminar but the fluid inertia effect cannot be neglected, the classical Reynolds equation is not valid in such case.

Keeping in view of the above, consideration of inertia effect of a lubricant flow may be one of the areas of recent extension of the classical lubrication theory. Among the few studies related to fluid inertia effects, Constatinescu and Galetuse [2] evaluated the momentum equations for laminar and turbulent flows by assuming the velocity profiles is not strongly affected by the inertia forces . Banerjee et.al [3] introduced an extended form of Reynolds equation to include the effect of fluid inertia, adopting an iteration scheme. Chen and Chen [4] obtained the steady-state characteristics of finite bearings including inertia effect using the formulation of Banerjee et al.[3]. Tichy and Bou-said [5] and Kakoty and Majumdar [7] used the method of average inertia in which inertia terms are integrated over the film thickness to account for the inertia effect in their studies. The above studies were mainly based on ideally smooth bearing surfaces.

The effect of fluid inertia has been studied by many researchers for turbulent flow using long and short bearing approximations. However, there are few publications which deal only with the intermediate regime for finite oil journal bearings. Reinhardt and Lund [6] studied the dynamic characteristics based on first-order perturbation solution starting from the Navier-stokes equation. Banerjee et al.[3] introduced an extended form of Reynolds equation to include the effect of fluid inertia adopting an iteration scheme.

Kakoty and Majumdar [7- 8] carried out a first order perturbation technique in modified Reynolds number as was done by Reinhardt and Lund [6] for isoviscous fluid, to study the stability of an oil journal bearing.

In the present work, a modified average Reynolds equation and a solution algorithm are developed to include fluid inertia and pressure depended variable viscosity effects in the analysis of lubrication problems. The solutions of modified average Reynolds equations are obtained using finite difference method with appropriate iterative schemes.

An attempt is being made here to study the effect of fluid inertia with pressure dependent variable viscosity on the stability of oil film journal bearings under unidirectional constant load. The governing equations are deduced starting from the Navier-Stokes equation and flow continuity equations. These equations are identical (except for time dependent terms) to the ones developed by Constatinescu and Galetuse [2] which also include turbulent flow regime. In the present study the authors are particularly concerned with the laminar flow regime. An attempt is made to solve the system of nonlinear partial differential equation using Gauss-Siedel iteration method in a finite difference scheme.

A nonlinear time transient method is used to simulate the journal centre trajectory and to estimate the stability parameters.

II BASIC THEORY

The modified average Reynolds equation for fully lubricated surfaces is derived starting from the Navier-Stokes equations and the continuity equation with few assumptions. The schematic diagram of flexibly supported oil Journal Bearing is shown in Figure.1

The non-dimensional form of the momentum equations and the continuity equation for a journal bearing may be written as

$$R^*_e\left[\Omega\frac{\partial\bar{u}}{\partial\tau}+\bar{u}\frac{\partial\bar{u}}{\partial\theta}+\bar{v}\frac{\partial\bar{u}}{\partial\bar{y}}+\bar{w}\left(\frac{D}{L}\right)\frac{\partial\bar{u}}{\partial\bar{z}}\right]=-\frac{\partial\bar{p}}{\partial\theta}+\frac{\partial^2\bar{u}}{\partial\bar{y}^2} \quad (1)$$

$$\frac{\partial\bar{p}}{\partial\bar{y}}=0 \quad (2)$$

$$R^*_e\left[\Omega\frac{\partial\bar{w}}{\partial\tau}+\bar{u}\frac{\partial\bar{w}}{\partial\theta}+\bar{v}\frac{\partial\bar{w}}{\partial\bar{y}}+\bar{w}\left(\frac{D}{L}\right)\frac{\partial\bar{w}}{\partial\bar{z}}\right]=$$

$$-\left(\frac{D}{L}\right)\frac{\partial\bar{p}}{\partial\bar{z}}+\frac{\partial^2\bar{w}}{\partial\bar{y}^2} \quad (3)$$

$$\frac{\partial\bar{u}}{\partial\theta}+\frac{\partial\bar{v}}{\partial\bar{y}}+\left(\frac{D}{L}\right)\frac{\partial\bar{w}}{\partial\bar{z}}=0 \quad (4)$$

Where, $\bar{z}=\frac{z}{L/2}$, $\bar{y}=\frac{y}{c}$, $\theta=\frac{x}{R}$, $\tau=\omega_p.t$, $\Omega=\frac{\omega_p}{\omega}$,

$\bar{u}=\frac{u}{\omega R}$, $\bar{v}=\frac{v}{c\omega}$ $\bar{w}=\frac{w}{\omega R}$ $\bar{p}=\frac{pc^2}{\eta\omega R^2}$ and

$R_e^*=R_e.\frac{c}{R}=\frac{\rho\omega c^2}{\eta}$

The fluid film thickness can be given as

$$h=c+e\cos\theta \quad (5)$$

$$\bar{h}=1+\varepsilon\cos\theta \quad (6)$$

where, $\bar{h}=\frac{h}{c}$, $\varepsilon=\frac{e}{c}$,

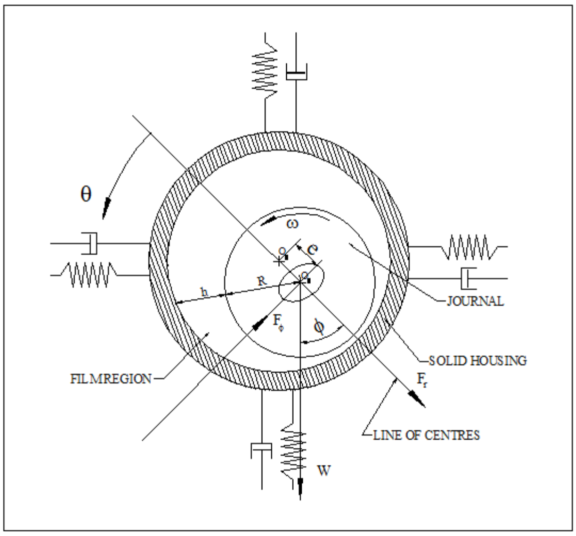

Fig.1 The schematic diagram of flexibly supported oil Journal Bearing

Here the variation in the density with time is considered to be negligible. The momentum equations may be presented in the following form using equation of continuity. However, the second momentum equation is not used any further because there is no variation in pressure across the film.After Constantinescu and Galetuse [2] the velocity components are approximated by the parabolic profiles. The velocity components may be expressed in non-dimensional form as follows:

$$\bar{u}=\left[\frac{\bar{y}}{\bar{h}}+Q_\theta\left(\frac{\bar{y}^2}{\bar{h}^2}-\frac{\bar{y}}{\bar{h}}\right)\right] \quad (7)$$

$$\bar{w}=\left[Q_z\left(\frac{\bar{y}^2}{\bar{h}^2}-\frac{\bar{y}}{\bar{h}}\right)\right] \quad (8)$$

Q_θ and Q_z are dimensionless flow parameter in θ and $\bar{z}$ direction respectively. Substituting these two into momentum equations and integrating give

$$Q_\theta=\frac{\bar{h}^2}{2}\left(\frac{\partial\bar{p}}{\partial\theta}\right)+R_e^*\times I_X \quad (9)$$

$$Q_z=\frac{\bar{h}^2}{2}\left(\frac{D}{L}\right)\left(\frac{\partial\bar{p}}{\partial\bar{z}}\right)+R_e^*\times I_Z \quad (10)$$

where,

$$I_X=\frac{\bar{h}}{2}\left[\frac{1}{2}\Omega\left(1-\frac{1}{3}Q_\theta\right)\frac{\partial\bar{h}}{\partial\tau}-\frac{1}{6}\Omega\bar{h}\frac{\partial Q_\theta}{\partial\tau}-\frac{1}{3}\left(1-\frac{1}{2}Q_\theta+\frac{1}{10}Q_\theta^{\,2}\right)\frac{\partial\bar{h}}{\partial\theta}+\right.$$

$$\left.\frac{1}{3}\bar{h}\left(\frac{1}{5}Q_\theta-\frac{1}{2}\right)\frac{\partial Q_\theta}{\partial\theta}+\frac{1}{30}\left(\frac{D}{L}\right)\bar{h}Q_z\frac{\partial Q_\theta}{\partial\bar{z}}+\frac{1}{6}\left(\frac{D}{L}\right)\bar{h}\left(\frac{1}{5}Q_\theta-\frac{1}{2}\right)\frac{\partial Q_z}{\partial\bar{z}}\right] \quad (11)$$

$$I_Z=\frac{\bar{h}}{2}\left[-\frac{1}{6}\Omega Q_z\frac{\partial\bar{h}}{\partial\tau}-\frac{1}{6}\Omega\bar{h}\frac{\partial Q_z}{\partial\tau}-\frac{1}{6}Q_z\left(\frac{1}{5}Q_\theta-\frac{1}{2}\right)\frac{\partial\bar{h}}{\partial\theta}-\right.$$

International Journal of Engineering Research & Technology (IJERT)
ISSN: 2278-0181
Vol. 10 Issue 01, January-2021

$$\frac{1}{6}\bar{h}\left(\frac{1}{5}Q_\theta-\frac{1}{2}\right)\frac{\partial Q_z}{\partial \theta}+\frac{1}{30}\bar{h}Q_z\frac{\partial Q_\theta}{\partial \theta}+\frac{1}{15}\left(\frac{D}{L}\right)\bar{h}\,Q_z\frac{\partial Q_z}{\partial \bar{z}}\Bigg] \quad (12)$$

Considering case of variable viscosity it has been observed oils viscosity increases with pressure and the following relationship is assumed similar to Majumdar et.al. [9],

$$\eta=\eta_0 e^{\alpha p} \quad (13)$$

Where α = piezo viscosity co-efficient, η_0 Viscosity of oil at the inlet condition

Assuming modified pressure function q we get

$$q=\frac{1}{\alpha}(1-e^{-\alpha p}) \quad (14)$$

Considering time dependent terms one can obtain the following form of modified Reynold's equation for dynamic condition considering fluid inertia effect.

$$\frac{\partial}{\partial\theta}\left(\bar{h}^3\frac{\partial \bar{q}}{\partial\theta}\right)+\left(\frac{D}{L}\right)^2\frac{\partial}{\partial \bar{z}}\left(\bar{h}^3\frac{\partial \bar{q}}{\partial \bar{z}}\right)=$$

$$12\,\Omega\frac{\partial \bar{h}}{\partial \tau}+6\left(1.0-2.0\,\Omega\frac{\partial \phi}{\partial \tau}\right)\frac{\partial \bar{h}}{\partial \theta} \quad (15)$$

Where, $\bar{q}=\dfrac{q c^2}{\eta_0\omega R^2}$

and

$$Q_\theta=\frac{\bar{h}^2}{2}\left(\frac{\partial \bar{q}}{\partial \theta}\right)+R_e^*\times I_X \quad (16)$$

$$Q_z=\frac{\bar{h}^2}{2}\left(\frac{D}{L}\right)\left(\frac{\partial \bar{q}}{\partial \bar{z}}\right)+R_e^*\times I_Z \quad (17)$$

Where, I_x and I_z are same as equation (11) and (12) above.

Boundary conditions for equation (15) are as follows

1. The pressure at the ends of the bearing is assumed to be zero (ambient): $\bar{q}(\theta,\pm 1)=0$
2. The pressure distribution is symmetrical about the mid-plane of the bearing: $\dfrac{\partial \bar{q}}{\partial \bar{z}}(\theta,0)=0$
3. Cavitation boundary condition is given by: $\dfrac{\partial \bar{q}}{\partial \theta}\left(\theta_2,\bar{z}\right)=0$ *and* $\bar{q}\left(\theta,\bar{z}\right)=0$ *for* $\theta\geq\theta_2$

Where θ_2 is the angular coordinate at which the film cavitates.

Now from equation (14) p can be written in terms of q as

$$p=-\frac{\ln(1-\alpha\,q)}{\alpha}$$

After non-dimensionalised the relation can be given as

$$\bar{p}=\frac{\ln(1-\xi\,\bar{q})}{\xi} \quad (18)$$

Where, viscosity parameter, $\xi=\dfrac{\eta_0\alpha\omega R^2}{c^2}$

The equations (6), (11), (12),(15), (16) and (17) are first expressed in finite difference form and solved using Gauss-Siedel method in a finite difference scheme.

III METHOD OF SOLUTION

To find out steady-state pressure all the time derivatives are set equal to zero and Equations. (6), (11),(12),(15),(16)and(17) are solved simultaneously.

For $\varepsilon\leq 0.2$ the pressure distribution and flow parameters Q_θ and Q_z are evaluated from inertia less (i.e, $R_e^*=0$) solution, i.e., solving classical Reynold's equation. These values are then used as initial value of flow parameters to solve equations (16) and (17) simultaneously for Q_θ and Q_z using Gauss-Siedel method in a finite difference scheme. Then update I_x & I_z and then again calculate Q_θ and Q_z with modified value I_x & I_z for use to solve Equation (15) for new modified pressure $\bar{q}$ considering inertia effect with pressure dependent variable viscosity by using a successive over relaxation scheme. The latest values of Q_θ and Q_z and $\bar{q}$ are used iteratively to solve the set of equations until all variables converges. The convergence criterion adopted for pressure is $\left[1-\sum\bar{q}_{new}\Big/\sum\bar{q}_{old}\right]\leq 10^{-5}$ and also same criterion for Q_θ and Q_z.

For higher eccentricity ratios ($\varepsilon>0.2$) the initial values for the variables are taken from the results corresponding to the previous eccentricity ratios.

Very small increment in ε is to be provided as Re^* increases. The procedure converges up to a value of $Re^*=1.4$ which should be good enough for the present study. After getting $\bar{q}$ solving the above equations simultaneously the $\bar{q}$ is then converted to $\bar{p}$ using equation (18) to calculate fluid film pressures for a particular value of viscosity parameter.

Since the bearing is symmetrical about its central plane ($\bar{z}$ =0),only one half of the bearing needs to be considered for the analysis, Once the pressure distribution is evaluated fluid film forces and the load bearing capacity $\bar{W}_o$ and attitude angle (φ) are calculated as follows:

A. *Fluid film forces*

The non-dimensional fluid film forces along line of centers and perpendicular to the line of centers are given by

$$\bar{F}_r\left(=\frac{F_r C^2}{\eta\,\omega R^3 L}\right)=\int_0^1\int_{\theta_1}^{\theta_2}\bar{p}\cos\theta\,d\theta\,d\bar{z} \qquad (19)$$

$$\bar{F}_\phi\left(=\frac{F_\phi C^2}{\eta\,\omega R^3 L}\right)=\int_0^1\int_{\theta_1}^{\theta_2}\bar{p}\sin d\theta\,d\bar{z} \qquad (20)$$

where θ_1 and θ_2 are angular coordinates at which the fluid film commences and cavitates respectively.

B. *Steady state load*

The steady state non-dimensional load and attitude angle are given by

$$\bar{W}_0=\sqrt{\left(\bar{F}_{r_0}{}^2+\bar{F}_{\phi_0}{}^2\right)} \qquad (21)$$

$$\phi_o=\tan^{-1}\left(\frac{-\bar{F}_{\phi_0}}{\bar{F}_{r_0}}\right) \qquad (22)$$

Since the steady state film pressure distribution has been obtained at all the mesh points, integration of equations (19) and (20) can be easily performed numerically by using Simpson's 1/ 3 rd. rule to get $\bar{F}_r$ and $\bar{F}_\phi$. The steady state load $\bar{W}_0$ and the attitude angle (ϕ_0) are calculated using equations (21) and (22).

C. *Equation of Motion*

The figure 2 shows the Coordinate system in oil journal bearing and figure 3 shows the hydrodynamic fluid film forces in circumferential & radial direction of the bearing geometrics.

The equation of motion for a rigid rotor supported on four identical flexibly supported bearings are given by,

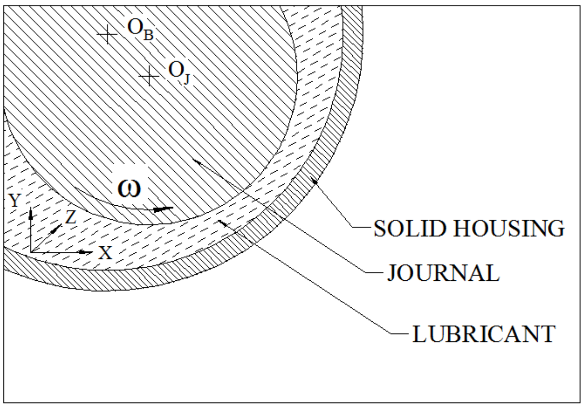

Fig. 2: Coordinate system in oil journal bearing

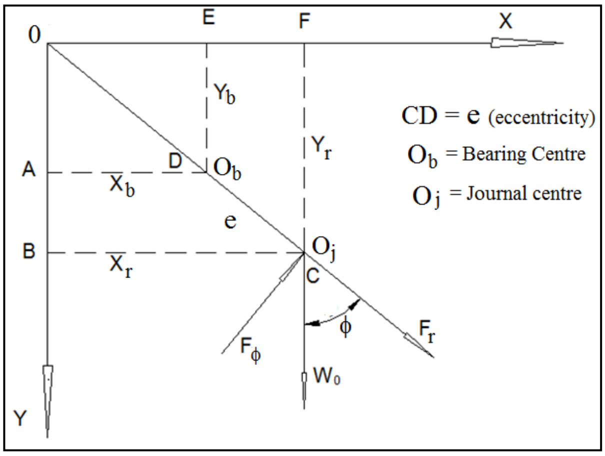

Fig. 3: Hydrodynamic fluid film forces in circumferential & radial direction

$$M_r.\frac{d^2X_r}{dt^2}=F_r\sin\phi+F_\phi\cos\phi \qquad (23)$$

$$M_r.\frac{d^2Y_r}{dt^2}=F_r\cos\phi-F_\phi\sin\phi+W_0 \qquad (24)$$

$$M_b.\frac{d^2X_b}{dt^2}=-F_\phi\cos\phi-F_r\sin\phi-B.\frac{dX_b}{dt}-KX_b \qquad (25)$$

$$M_b.\frac{d^2Y_b}{dt^2}=F_\phi\sin\phi-F_r\cos\phi-B.\frac{dY_b}{dt}-KY_b \qquad (26)$$

The relation between rotor & bearing motion are given by,

$$X_r=X_b+e\sin\phi \qquad (27)$$

$$Y_r=Y_b+e\cos\phi \qquad (28)$$

The above two equations are substituted in equations of motion. Finally the equations of motion are expressed in non-dimensional form as follows,

$$\dot{\bar{X}}_b=\frac{d\bar{X}_b}{d\tau} \qquad (29)$$

$$\dot{\bar{Y}}_b=\frac{d\bar{Y}_b}{d\tau} \qquad (30)$$

$$\ddot{\bar{X}}_b=\frac{1}{m.\bar{M}.\bar{W}_0.\Omega^2}\left[-\bar{F}_\phi\cos\phi-\bar{F}_r\sin\phi-\Omega.\bar{W}_0.\bar{B}.\dot{\bar{X}}_b-\bar{W}_0.\bar{K}.\bar{X}_b\right] \qquad (31)$$

$$\ddot{\bar{Y}}_b=\frac{1}{m.\bar{M}.\bar{W}_0.\Omega^2}\left[\bar{F}_\phi\sin\phi-\bar{F}_r\cos\phi-\Omega.\bar{W}_0.\bar{B}.\dot{\bar{Y}}_b-\bar{W}_0.\bar{K}.\bar{Y}_b\right] \qquad (32)$$

$$\dot{\varepsilon}=\frac{d\varepsilon}{d\tau} \qquad (33)$$

$$\dot{\phi}=\frac{d\phi}{d\tau} \qquad (34)$$

$$\ddot{\varepsilon}=\frac{A_3.F-A_4.E}{A_2.A_3-A_1.A_4} \qquad (35)$$

$$\ddot{\phi}=\frac{A_2.E-A_1.F}{A_2.A_3-A_1.A_4} \qquad (36)$$

where,

$$C=-2\dot{\varepsilon}.\dot{\phi}\cos\phi+\varepsilon.\sin\phi.\left(\dot{\phi}\right)^2+\frac{1}{\bar{M}.\bar{W}_0.\Omega^2}\left[\bar{F}_r\sin\phi+\bar{F}_\phi\cos\phi\right]$$

International Journal of Engineering Research & Technology (IJERT)
ISSN: 2278-0181
Vol. 10 Issue 01, January-2021

$$D = 2\dot{\varepsilon}.\dot{\phi}.\sin\phi + \varepsilon.\cos\phi.\left(\dot{\phi}\right)^2 +$$

$$\frac{1}{\bar{M}.\overline{W}_0.\Omega^2}\left[\overline{F}_r\cos\phi - \overline{F}_\phi\sin\phi + \overline{W}_0\right]$$

$$A_1 = \sin\phi,\ A_2 = \cos\phi,\ A_3 = \varepsilon.\cos\phi,$$

$$A_4 = -\varepsilon.\sin\phi$$

$$G = \ddot{\overline{X}}_b$$

$$H = \ddot{\overline{Y}}_b$$

$$E = C - G$$

$$F = D - H$$

D. *Solution Scheme*:

For stability analysis, a non-linear time transient analysis is carried out using the equations of motion to compute a new set of $\varepsilon, \phi, X_b, Y_b$ & their derivatives for the next time step for a given set of. Re*, L/D, ε_0, $\bar{M}$ (Mass parameter) for a particular Viscosity parameter ξ. The forth order Runge-Kutta method is used for solving the equations of motion. The hydrodynamic forces are computed for every time step by solving the partial differential equation for pressure satisfying the boundary conditions.

Stability Analysis

To study the effect of fluid inertia with pressure dependent variable viscosity on journal center trajectory of flexibly supported bearings a set of trajectories of journal center and bearing has been studied and it is possible to construct the trajectories for numbers of complete revolution of the journal the plots shows the stability of the journal when the trajectory of journal and bearing center ends in a limit cycle. Critical mass parameter for a particular eccentricity ratio, slenderness ratio, modified Reynold's number, viscosity parameter and roughness pattern is found when the trajectories ends with limit cycle (Fig. 18 & Fig.19) or it changes its trend from stable to unstable.

IV RESULTS AND DISCUSSION

Steady state analysis

The steady-state analysis was done and its results are compared to the results of Kakoty et.al., [7] and Chen and Chen [4], for (for L/D = 1.0) as given in Table 1. These two results are in good agreement. A slight decrease in load capacity with modified Reynolds number (Re*) is observed in the present study. In the present study it is observed that the attitude angle increases slightly for most of the eccentricity ratios up to $\varepsilon_0 \leq 0.8$.

Table 1: Comparison of Steady - state characteristics of a finite iso-viscous oil journal bearings for L/D=1 with fluid Inertia Effect.

Re*	ε_0	$\bar{W}_0$	$\bar{W}_0$	$\bar{W}_0$	ϕ_0	ϕ_0	ϕ_0
		Present	Kakoty	Chen-Chen	Present	Kakoty	Chen-Chen
0	0.2	0.5031	0.5042	0.501	77.541	73.710	73.900
	0.5	1.7592	1.7903	1.779	58.398	56.640	56.800
	0.8	7.0854	7.4597	7.146	36.345	34.660	36.200
	0.9	16.891	17.713	16.982	26.175	23.900	26.400
0.28	0.2	0.5043	0.5055	0.504	77.927	73.750	74.200
	0.5	1.7940	1.7980	1.785	57.725	56.720	57.000
	0.8	7.1942	7.4837	7.151	36.310	34.720	36.300
	0.9	17.043	17.761	16.993	26.240	23.930	26.400
0.56	0.2	0.5055	0.5070	0.505	78.311	73.790	74.500
	0.5	1.8296	1.8058	1.790	57.114	56.790	57.200
	0.8	7.3013	7.5081	7.159	36.291	34.780	36.400
	0.9	17.191	17.8090	17.002	26.308	23.970	26.400
1.4	0.2	0.5092	0.5112	0.5086	79.4491	73.950	75.300
	0.5	1.9345	1.8307	1.5870	55.4596	57.050	58.000
	0.8	7.6098	7.5852	7.1870	36.2559	35.020	36.700
	0.9	17.6245	------	17.0300	26.5092	----	26.600

Stability analysis

There are limited publications which deal only with the non linear stability analysis for finite oil journal bearings with flexibly support. Kakoty and Majumdar [7] studied the nonlinear stability of flexibly supported oil journal bearing with the effect of fluid inertia only with isoviscous fluid but did not provide any tables for comparison. Observed the nature / trend of the curves are quite similar with present study. Below figure shows in both the cases with same parameter values the trend of the trajectory is towards Point stability.

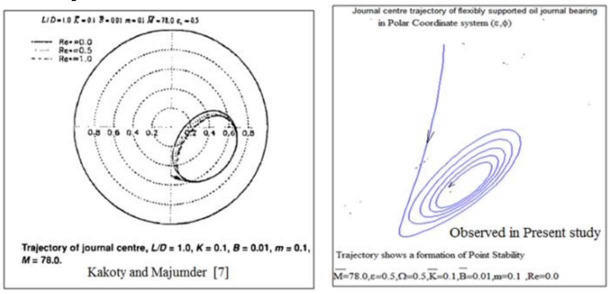

Figure 4: Comparison the nature of curve

A. *Effect of modified Reynolds number with eccentricity ratio.*

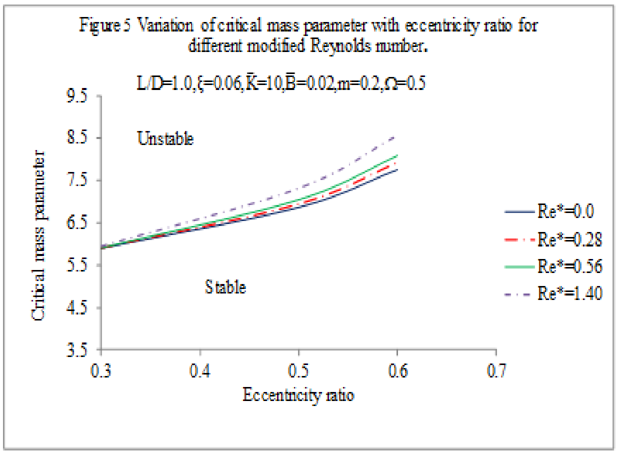

Figure 5 Variation of critical mass parameter with eccentricity ratio for different modified Reynolds number.

International Journal of Engineering Research & Technology (IJERT)
ISSN: 2278-0181
Vol. 10 Issue 01, January-2021

Figure 5 shows the variation of critical mass parameter with eccentricity ratio for different modified Reynold's number. It is observed that critical mass parameter increases with the increase in eccentricity ratio and increase of modified Reynold's number. The increasing trend is high for $\varepsilon \geq 0.5$ and $R_e^* = 1.40$

B. *Effect of eccentricity ratio with modified Reynold's number*

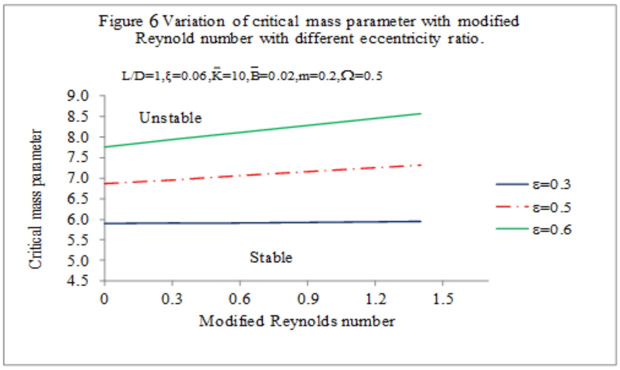

Figure 6 Variation of critical mass parameter with modified Reynold number with different eccentricity ratio.

Figure 6 shows the variation of critical mass parameter with the modified Reynold's number for different eccentricity ratio. It is observed that critical mass parameter increases with the increase of modified Reynold's number for eccentricity ratio ($\varepsilon \geq 0.5$) and variation remain almost constant for $\varepsilon = 0.3$

C. Effect of slenderness ratio with eccentricity ratio.

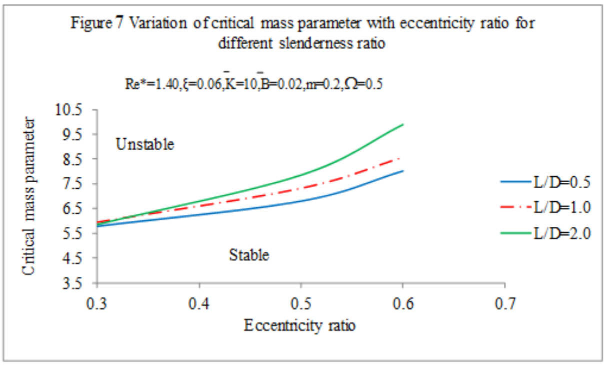

Figure 7 Variation of critical mass parameter with eccentricity ratio for different slenderness ratio

Figure 7 shows the variation of critical mass parameter with eccentricity ratio for different slenderness ratio. It is observed that critical mass parameter increases with eccentricity ratio and also as the slenderness ratio increases and the variation nature can be observed from the figure 7.

D.*Effect of eccentricity ratio with slenderness ratio*

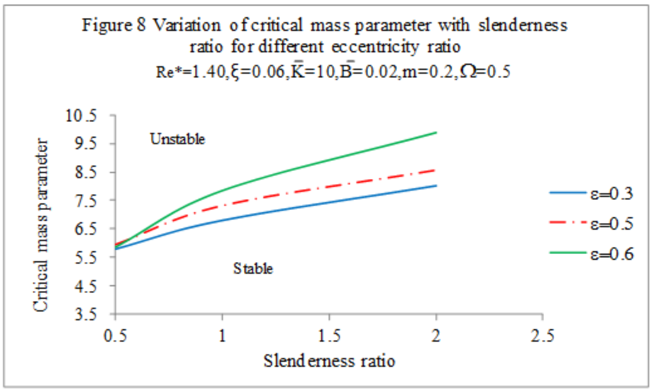

Figure 8 Variation of critical mass parameter with slenderness ratio for different eccentricity ratio

Figure 8 shows the variation of critical mass parameter with slenderness ratio for different eccentricity ratio. It is observed that critical mass parameter increases with the increase of slenderness ratio and also with the increase of eccentricity ratio.

E. Effect of modified Reynold's number with slenderness ratio

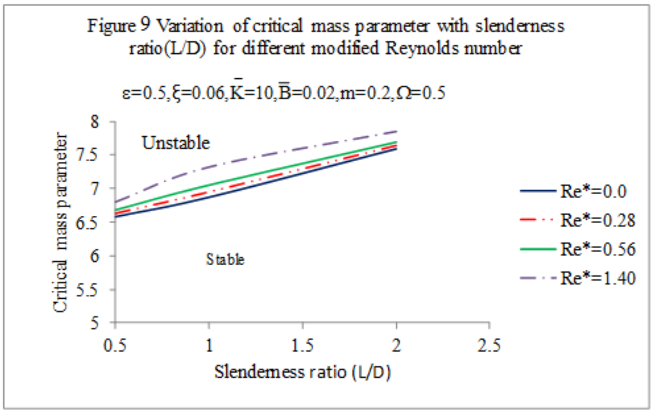

Figure 9 Variation of critical mass parameter with slenderness ratio(L/D) for different modified Reynolds number

Figure 9 shows the variation of critical mass parameter with slenderness ratio for different modified Reynold's number. It is observed critical mass parameter increases with slenderness ratio and also with the increase of modified Reynold's number. The nature of variation can be observed from the figure 9.

F. Effect of slenderness ratio with modified Reynold's number.

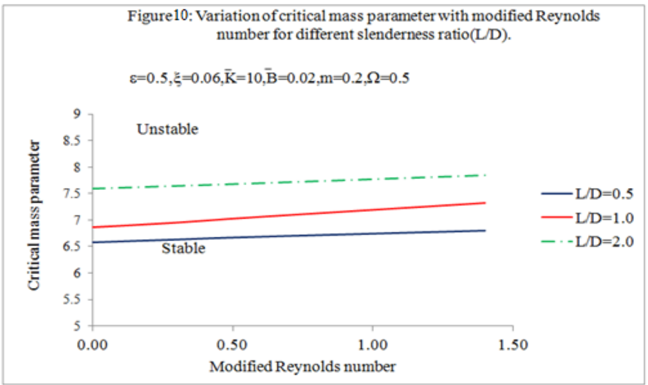

Figure10: Variation of critical mass parameter with modified Reynolds number for different slenderness ratio(L/D).

Figure 10 shows the variation of critical mass parameter with modified Reynold's number for different slenderness ratio. It is observed critical mass parameter remain almost constant with R_e^* although slight increase is noticed for $L/D = 1.0$

International Journal of Engineering Research & Technology (IJERT)
ISSN: 2278-0181
Vol. 10 Issue 01, January-2021

G.*Effect of viscosity parameter with eccentricity ratio*

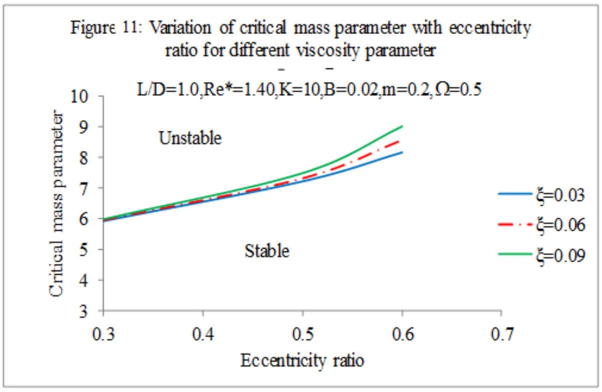

Figure 11 shows the variation of critical mass parameter with eccentricity ratio for different viscosity parameter .It is observed that critical mass parameter increases with the increase of eccentricity ratio and also with increase of viscosity parameter.

H. Effect of viscosity parameter with modified Reynold's number

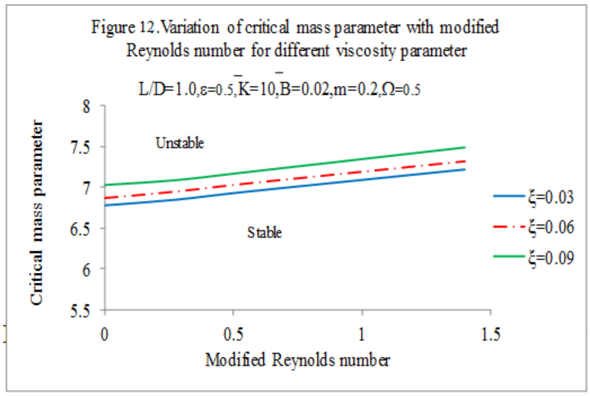

Figure 12 shows the variation of critical mass parameter with modified Reynold's number for different viscosity parameter. It is observed that critical mass parameter increases linearly with R_e^* and with the increase of viscosity parameter ξ.

I. *Effect of stiffness coefficient with eccentricity ratio*

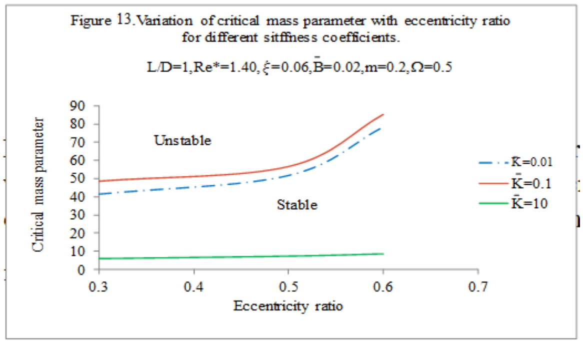

Figure 13 shows the variation of critical mass parameter with eccentricity ratio for different stiffness coefficient. It is observed critical mass parameter increases with increase of eccentricity ratio. The trend of increase is more prominent for $\varepsilon \geq 0.5$ and $\overline{K} \leq 0.1$

J. *Effect of damping coefficient with eccentricity ratio*

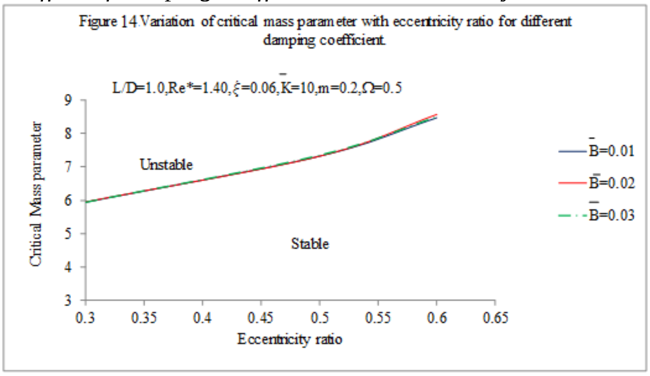

Figure 14 shows the variation of critical mass parameter with eccentricity ratio for different damping coefficient. It is observed that the variation of critical mass parameter is insignificant for different damping coefficient $\bar{B}$

K Effect of slenderness ratio with viscosity parameter

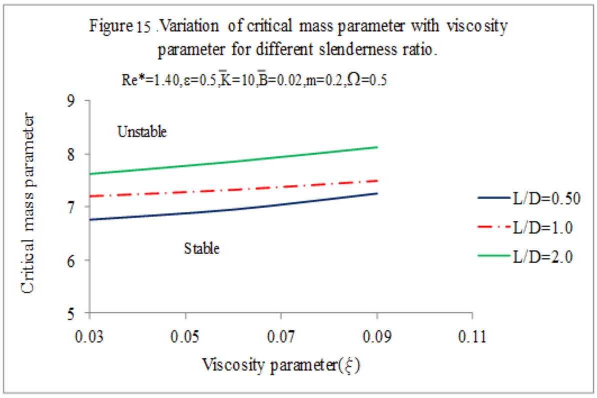

Figure 15 shows the variation of critical mass parameter with viscosity parameter for different slenderness ratio. It is observed that critical mass parameter increases linearly with viscosity parameter and with the increase of slenderness ratio.

L. Effect of viscosity parameter with slenderness ratio

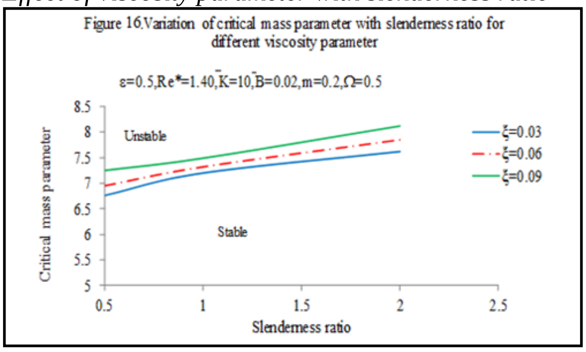

Figure 16 shows the variation of critical mass parameter with slenderness ratio for different viscosity coefficient. It is observed that critical mass parameter increases linearly with slenderness ratio and with the increase of viscosity parameter ξ.

M. comparison of variable viscosity and iso-viscous lubricants.

International Journal of Engineering Research & Technology (IJERT)
ISSN: 2278-0181
Vol. 10 Issue 01, January-2021

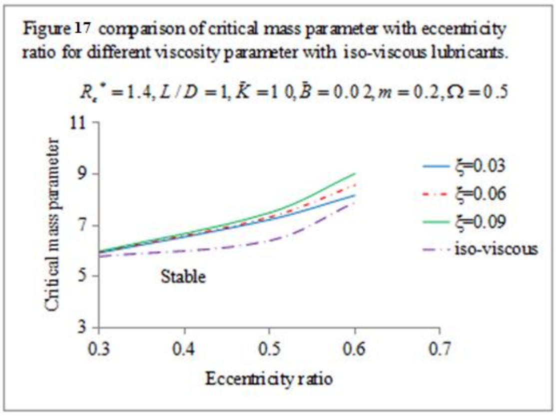

Figure 17 comparison of critical mass parameter with eccentricity ratio for different viscosity parameter with iso-viscous lubricants.

Figure 17 shows the comparison of critical mass parameter between pressure dependent variable viscosity and iso-viscous lubricant for different viscosity parameter for R_e^*=1.4 and L/D=1.0. It is observed that the critical mass increases with the increase in eccentricity ratio for all the viscosity observed for all the viscosity parameter compared to iso-viscous lubricants and the increase is more for $\varepsilon \geq 0.5$ and $\xi = 0.09$.

N. Journal centre trajectory (Limit cycle)

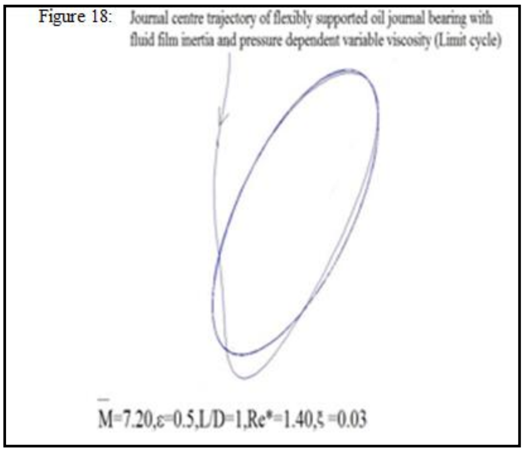

Figure 18: Journal centre trajectory of flexibly supported oil journal bearing with fluid film inertia and pressure dependent variable viscosity (Limit cycle)

Figure 18. Journal Center trajectory (Limit cycle)

O. Bearing centre trajectory(Limit cycle)

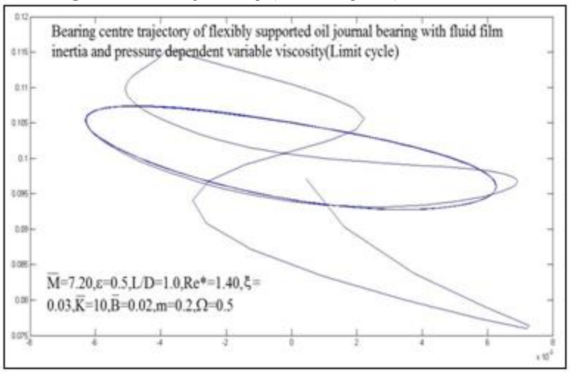

Bearing centre trajectory of flexibly supported oil journal bearing with fluid film inertia and pressure dependent variable viscosity(Limit cycle)

Figure 19. Bearing Center trajectory (Limit cycle)

P. Variation of whirl ratio with eccentricity ratio for different viscosity parameter

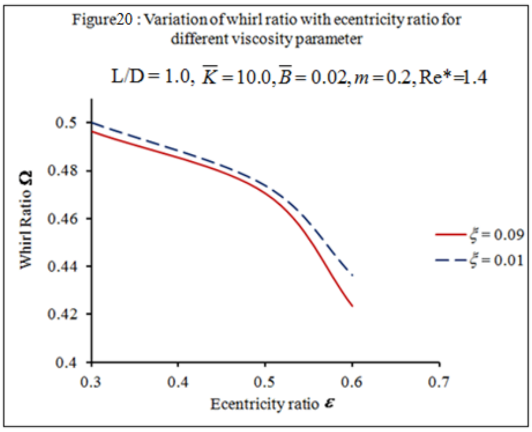

Figure20 : Variation of whirl ratio with eccentricity ratio for different viscosity parameter

Figure 20 shows the variation of whirl ratio with eccentricity ration for different viscosity parameter ξ. It is observed that whirl ratio decreases with increase of eccentricity ratio and also with the increase of viscosity parameter ξ.

V CONCLUSIONS

(i) Stability increases with the increase of eccentricity ratio and with the increase of modified Reynold's number and with the increase in slenderness ratio and also increase of viscosity parameter.
(ii) Stability increases with the increase in eccentricity ratio and decrease with the increase in stiffness coefficient.
(iii) Stability is unaffected due to increase in eccentricity ratio and damping coefficient.
(iv) whirl ratio decreases with increase of eccentricity ratio and also with the increase of viscosity parameter

VI NOMENCLATURE

c = Radial clearance (m)
D = Diameter of Journal (m)
e = eccentricity (m)
F_{r_0}, F_{ϕ_0} = Steady state hydrodynamic film forces (N).
$\bar{F}_{r_0}, \bar{F}_{\phi_0}$ = Dimensionless steady state hydrodynamic film forces
h = Film thickness, (m)
$\bar{h}$ = Dimensionless film thickness, h/c
L = Length of the bearing in m
p = Film pressure in Pa
$\bar{p}$ = dimensionless film pressure = $\left(\frac{pc^2}{\eta\omega R^2}\right)$
R = radius of journal in m
R_e = Reynolds number, $\frac{\rho c R\omega}{\eta}$
R^*_e = Modified Reynolds number, $\left(\frac{c}{R}\right)R_e$
t = time in s
$u, v\ w$ = velocity components in x, y, z directions in m/s.
$\bar{u}, \bar{v}, \bar{w}$ = dimensionless velocity components
W_0 = steady-state load bearing capacity in N

$\overline{W_0}$ = Dimensionless steady-state load $\frac{W_0 c^2}{\eta\omega R^3 L}$

x, y, z = coordinates

$\theta, \bar{Y}, \bar{Z}$ = Dimensionless coordinates, x/R, y/c, $z/L/2$

$\varepsilon, \varepsilon_0$ = Eccentricity ratio e/c (dimensionless),steady-state eccentricity ratio

ρ = Density of the lubricant (kg m^{-3})

ω = Angular velocity of journal(rad s^{-1})

ω_p = Angular velocity of whirl (rad s^{-1})

Ω = Whirl ratio, $\frac{\omega_p}{\omega}$

η_0 = Absolute viscosity of lubricating film at inlet condition (N s m^{-1})

ϕ = Attitude angle

Q_θ = Dimensionless flow parameter in θ direction

Q_z = Dimensionless flow parameter in $\bar{z}$ direction

$\bar{Q}$ = Dimensionless side leakage

θ_1, θ_2 = Angular coordinates at which film commences and cavitates.

$\xi = \frac{\eta_0 \alpha \omega R^2}{c^2}$ = Viscosity Parameter

VII REFERENCES

[1] Pinkus, O. and Sternlicht, B., *Theory of Hydrodynamic Lubrication*, New York, McGraw-Hill (1961).

[2] V. N. Constantinescu and S. Galetuse "On the Possibilities of Improving the Accuracy of the Evaluation of Inertia Forces in Laminar and Turbulent Films" *J. Tribol.* Vol 96 (1), 69-77 (Jan 01, 1974) (9 pages), ASME, Journal of Tribology , Volume 96,Issue 1.

[3] Banerjee Mihir B.,Shandil R.G.,and Katyal S.P.A "Nonlinear Theory of Hydrodynamic Lubrication"Journal of Mathematical Analysis and Applications 117,48-56(1986)

[4] Chen, C.H. and Chen, C.K., "The influence of fluid inertia on the operating characteristics of finite journal bearings", Wear, Vol. 131, (1989), pp. 229-240.

[5] Tichy, J., and Bou-Said, B., 1991, "Hydrodynamic Lubrication and Bearing Behavior with Impulsive Loads," STLE Tribol. Trans., 34, pp. 505–512.

[6] E. Reinhardt and J. W. Lund "*The Influence of Fluid Inertia on the Dynamic Properties of Journal Bearings*", Journal of Lubrication Technology, Volume 97 , Issue 2, 159-165, 1975.

[7] Kakoty S. K. and Majumdar B. C., "*Effect of Fluid Inertia on Stability of Oil Journal Bearing". ASME Journal of Tribology"*, Vol 122, pp 741-745, October 2000.

[8] Kakoty, S.K., Majumdar, B.C.: *Effect of fluid inertia on the dynamic coefficients and stability of journal bearings*, Proc. Inst. Mech. Engrs., Vol. 214-J, (2000) 229-242

[9] B.C.Majumder, D.E.Brewe and M.M.Khonsari, "Stability of a rigid rotor supported on flexible oil Journal bearings," Journal of Tribology Trans Vol 110, 1988, pp 181 - 187.